Small-x Asymptotics of the Quark Helicity Distribution

Yuri V. Kovchegov,[1,*] Daniel Pitonyak,[2,3,†] and Matthew D. Sievert[4,5,‡]
[1]Department of Physics, The Ohio State University, Columbus, Ohio 43210, USA
[2]Division of Science, Penn State University-Berks, Reading, Pennsylvania 19610, USA
[3]RIKEN BNL Research Center, Brookhaven National Laboratory, Upton, New York 11973, USA
[4]Theoretical Division, Los Alamos National Laboratory, Los Alamos, New Mexico 87545, USA
[5]Physics Department, Brookhaven National Laboratory, Upton, New York 11973, USA
(Received 1 November 2016; published 30 January 2017)

We construct a numerical solution of the small-x evolution equations derived in our recent work [J. High Energy Phys. 01 (2016) 072.] for the (anti)quark transverse momentum dependent helicity TMDs and parton distribution functions (PDFs) as well as the g_1 structure function. We focus on the case of large N_c, where one finds a closed set of equations. Employing the extracted intercept, we are able to predict directly from theory the behavior of the quark helicity PDFs at small x, which should have important phenomenological consequences. We also give an estimate of how much of the proton's spin carried by the quarks may be at small x and what impact this has on the spin puzzle.

DOI: 10.1103/PhysRevLett.118.052001

Introduction.—For many decades, it has been known that the proton is a complex object composed of quarks, antiquarks, and gluons (collectively called partons). The properties of the proton are thus emergent phenomena arising from the dynamics of partons. For example, the spin of the proton ($= 1/2$ in units of $\hbar$), which is one of its most fundamental quantum numbers, should be a sum of the spin and orbital angular momentum (OAM) of its partons. This can be expressed in terms of helicity sum rules [1–4], like that of Jaffe and Manohar [1]

$$S_q + L_q + S_G + L_G = \frac{1}{2}, \tag{1}$$

where S_q and S_G are the spin of the quarks and gluons, respectively, while L_q and L_G denote their OAM. The quantities S_q and S_G are defined as the following integrals over Bjorken x at a fixed momentum scale Q^2:

$$S_q(Q^2) = \frac{1}{2}\int_0^1 dx\, \Delta\Sigma(x, Q^2), \tag{2}$$

$$S_G(Q^2) = \int_0^1 dx\, \Delta G(x, Q^2), \tag{3}$$

with

$$\Delta\Sigma(x, Q^2) = [\Delta u + \Delta\overline{u} + \Delta d + \Delta\overline{d} + \cdots](x, Q^2), \tag{4}$$

where the helicity parton distribution functions (PDFs) for a parton of flavor $f = u, \overline{u}, d, \overline{d}, \ldots, G$ are denoted by Δf. These are equal to the number density of partons with the same helicity as the proton minus the number density of those with opposite helicity.

In the late 1980s, the community was largely surprised when the European Muon Collaboration (EMC) measured S_q to be a significantly smaller fraction of the proton's spin than had been naïvely expected [6,7]. This result led to the spin puzzle centered around the question of how the pieces in Eq. (1) add up to $1/2$. To help pin down another term in this sum, there has been intense effort over the last decade to measure and extract S_G. Recent experiments show that S_G can give a more substantial fraction of the proton's spin than once thought [8,9]. The current quark and gluon spin values extracted from the experimental data are $S_q(Q^2 = 10\ \mathrm{GeV}^2) \approx 0.15$–$0.20$ (integrated over $0.001 < x < 1$) and $S_G(Q^2 = 10\ \mathrm{GeV}^2) \approx 0.13$–$0.26$ (integrated over $0.05 < x < 1$) [10]. One option, then, is that the rest of the proton's spin is due to quark and gluon OAM. However, note that the quoted values for S_q and S_G are for integrals over a truncated range $x_{\min} < x < 1$ (where the relevant quantities are constrained by data), while the formulas in Eqs. (2), (3) involve integrals over the full range $0 < x < 1$. This leaves open the possibility that there could be significant quark and gluon spin at small x, which is the scenario we explore in this Letter.

The use of the small-x formalism to analyze quark polarization was pioneered decades ago by Kirschner and Lipatov [14] (see also [15–17]) and later by Bartels, Ermolaev, and Ryskin (herein referred to as BER) in the context of the structure function $g_1(x, Q^2)$ [18,19]. In particular, BER resummed double logarithms $\alpha_s \ln^2(1/x)$ using infrared evolution equations to predict a strong *growth* in $g_1(x, Q^2)$ at small x, a scenario that would have a major impact on the spin puzzle. In a recent work, we formulated the problem in a different language, which

employs light cone Wilson line operators and color dipoles [20–30], to derive evolution equations relevant for the [collinear and transverse momentum dependent (TMD)] helicity PDFs as well as the g_1 structure function [31].

In what follows, we solve these helicity evolution equations numerically (in the limit of a large number of colors N_c) in order to give a direct input from theory on the small-x behavior of helicity PDFs, which should have important phenomenological consequences. We extract the high-energy intercept α_h to predict the small-x asymptotics of $\Delta\Sigma(x,Q^2) \sim (1/x)^{\alpha_h}$ and estimate how much of the proton's spin carried by the quarks one can expect to find at low x.

The helicity evolution equations.—As shown in [32], at small x the quark helicity PDF in the flavor-singlet case $\Delta q^S(x,Q^2)$ [and, therefore, $\Delta\Sigma(x,Q^2)$] can be written in terms of the impact-parameter integrated polarized dipole amplitude $G(x_{10}^2,z)$ as [33]

$$\Delta q^S(x,Q^2) = \frac{N_c}{2\pi^3}\sum_f \int_{z_i}^1 \frac{dz}{z}\int_{\frac{1}{zs}}^{\frac{1}{zQ^2}} \frac{dx_{10}^2}{x_{10}^2} G(x_{10}^2,z). \quad (5)$$

Here $\underline{x}_{10} = \underline{x}_1 - \underline{x}_0$ is the dipole size, z is the fraction of the probe's longitudinal momentum carried by the softest (anti) quark in the dipole, $z_i = \Lambda^2/s$, with Λ an infrared (IR) momentum cutoff, and s is the center-of-mass energy squared. The singularity at $\underline{x}_{10} = 0$ is regulated by requiring that $x_{10} \equiv |\underline{x}_{10}| > 1/(zs)$, with $1/(zs)$ the shortest distance (squared) allowed in the problem.

To determine $G(x_{10}^2,z)$, we will solve the evolution equations derived in [31]. They resum powers of $\alpha_s \ln^2(1/x)$, which is the double-logarithmic approximation (DLA). Similar to the unpolarized case [20–30], helicity evolution equations do not close in general, forming a closed set only in the large-N_c and large-N_c & N_f limits (with N_f the number of flavors) [31]. Ignoring leading-logarithmic (LLA) saturation corrections [34], the large-N_c DLA evolution of $G(x_{10}^2,z)$ is governed by Eq. (83a) in [31] integrated over all impact parameters,

$$G(x_{10}^2,z) = G^{(0)}(x_{10}^2,z) + \frac{\alpha_s N_c}{2\pi}\int_{\frac{1}{x_{10}^2 s}}^{z}\frac{dz'}{z'}\int_{\frac{1}{z's}}^{x_{10}^2}\frac{dx_{21}^2}{x_{21}^2} \times [\Gamma(x_{10}^2,x_{21}^2,z') + 3G(x_{21}^2,z')]. \quad (6)$$

In Eq. (6), one also has the object $\Gamma(x_{10}^2,x_{21}^2,z')$, called a "neighbor" dipole amplitude [31]. The neighbor dipole obeys the (large-N_c, strictly DLA) evolution equation [31]

$$\Gamma(x_{10}^2,x_{21}^2,z') = \Gamma^{(0)}(x_{10}^2,x_{21}^2,z') + \frac{\alpha_s N_c}{2\pi}\int_{\frac{1}{x_{10}^2 s}}^{z'}\frac{dz''}{z''} \times \int_{\frac{1}{z''s}}^{\min\{x_{10}^2, x_{21}^2\frac{z'}{z''}\}}\frac{dx_{32}^2}{x_{32}^2}[\Gamma(x_{10}^2,x_{32}^2,z'') + 3G(x_{32}^2,z'')]. \quad (7)$$

Note that in Eqs. (6), (7) we have neglected small differences in the dipole sizes $x_{10}^2 \approx x_{20}^2 \approx x_{30}^2$. The solution to the simultaneous equations (6), (7), which we discuss in the next section, allows us to determine the small-x behavior of $G(x_{10}^2,z)$, and, hence, of $\Delta q^S(x,Q^2)$ in the dominant flavor singlet channel.

Numerical solution to the large-N_c evolution equations.—We start by defining new coordinates,

$$\eta \equiv \ln\frac{z}{z_i}, \quad \eta' \equiv \ln\frac{z'}{z_i}, \quad \eta'' \equiv \ln\frac{z''}{z_i}, \quad s_{10} \equiv \ln\frac{1}{x_{10}^2\Lambda^2}, \quad s_{21} \equiv \ln\frac{1}{x_{21}^2\Lambda^2}, \quad s_{32} \equiv \ln\frac{1}{x_{32}^2\Lambda^2}, \quad (8)$$

as well as rescaling all η's and s_{ij}'s,

$$\eta \to \sqrt{\frac{2\pi}{\alpha_s N_c}}\eta, \qquad s_{ij} \to \sqrt{\frac{2\pi}{\alpha_s N_c}}s_{ij}. \quad (9)$$

Using these variables, we write the large-N_c helicity evolution equations (6), (7) as

$$G(s_{10},\eta) = G^{(0)}(s_{10},\eta) + \int_{s_{10}}^{\eta} d\eta' \int_{s_{10}}^{\eta'} ds_{21} \times [\Gamma(s_{10},s_{21},\eta') + 3G(s_{21},\eta')] \quad (10a)$$

$$\Gamma(s_{10},s_{21},\eta') = \Gamma^{(0)}(s_{10},s_{21},\eta') + \int_{s_{10}}^{\eta'} d\eta'' \times \int_{\max\{s_{10}, s_{21}+\eta''-\eta'\}}^{\eta''} ds_{32}[\Gamma(s_{10},s_{32},\eta'') + 3G(s_{32},\eta'')]. \quad (10b)$$

Note that the ranges of the s_{21} and s_{32} integrations are restricted to positive values of s_{21} and s_{32} as long as s_{10} is positive; therefore, we always stay above the IR cutoff Λ (in momentum space). The initial conditions for Eqs. (10) are [32,35]

$$G^{(0)}(s_{10},\eta) = \Gamma^{(0)}(s_{10},s_{21},\eta) = \alpha_s^2\pi\frac{C_F}{N_c}[C_F\eta - 2(\eta - s_{10})], \quad (11)$$

with $C_F = (N_c^2-1)/(2N_c)$. Since the equations at hand are linear, and we are mainly interested in the high-energy intercept, we can scale out $\alpha_s^2\pi C_F/N_c$.

In order to solve Eqs. (10) [36], we first write down a discretized version of them

$$G_{ij} = G_{ij}^{(0)} + \Delta\eta\Delta s\sum_{j'=i}^{j-1}\sum_{i'=i}^{j'}[\Gamma_{ii'j'} + 3G_{i'j'}], \quad (12a)$$

$$\Gamma_{ikj} = \Gamma_{ikj}^{(0)} + \Delta\eta\Delta s\sum_{j'=i}^{j-1}\sum_{i'=\max\{i,k+j'-j\}}^{j'}[\Gamma_{ii'j'} + 3G_{i'j'}], \quad (12b)$$

where $G_{ij} \equiv G(s_i,\eta_j)$, $\Gamma_{ikj} \equiv \Gamma(s_i,s_k,\eta_j)$, and

$$\Delta\eta = \frac{\eta_{\max}}{N_\eta}, \qquad \Delta s = \frac{s_{\max}}{N_s}, \quad (13)$$

with $\eta_{\max}$ the maximum η value and N_η the number of grid steps in the η direction, and likewise, for $s_{\max}$, N_s. The discretized equations (12) are exact in the limit $\Delta\eta, \Delta s \to 0$ and $\eta_{\max}, s_{\max} \to \infty$. To optimize the numerics, we set $\eta_{\max} = s_{\max}$.

With the discretized evolution equations (12) in hand [along with the initial conditions (11) suitably discretized], we first choose values for $\eta_{\max} = s_{\max}$ and $\Delta\eta = \Delta s$. We then systematically go through the η-s grid in such a way that each G_{ij} (and Γ_{ijk}) only depends on G, Γ values that have already been calculated. Thus, we can determine G_{ij} for each i, j. Our numerical solution (for $\eta_{\max} = 40$, $\Delta\eta = 0.05$) is plotted in Fig. 1.

We next assume that in the high-energy limit

$$G(s_{10},\eta;\eta_{\max},\Delta\eta) \sim e^{\alpha_h(\eta_{\max},\Delta\eta)\eta + \beta_h(\eta_{\max},\Delta\eta)s_{10}} \quad (14)$$

with some coefficients α_h, β_h that are functions of $(\eta_{\max},\Delta\eta)$. We then fit $\ln[G(s_{01},\eta;\eta_{\max},\Delta\eta)]$ vs η for $s_{10} = 0$, using only $\eta \in [0.75\eta_{\max},\eta_{\max}]$. This allows us to extract the intercept $\alpha_h(\eta_{\max},\Delta\eta)$. We perform this procedure for $\eta_{\max} = 10$, 20, 30, 40, 50, 60, 70, and $\Delta\eta \in [\Delta\eta_{\min},0.1]$, where $\Delta\eta_{\min}$ is the smallest value of $\Delta\eta$, for a given $\eta_{\max}$, that is within our computational limits. The various intercepts we obtained are shown by the "data" points in Fig. 2.

As a last step, we extrapolate to the physical point $\eta_{\max} \to \infty$, $\Delta\eta \to 0$ by performing a two-dimensional fit to $\alpha_h(\eta_{\max},\Delta\eta)$, from which we can extract $\alpha_h(\eta_{\max} \to \infty, \Delta\eta \to 0) \equiv \alpha_h$ (see Fig. 2). In the end, we obtain $\alpha_h = 2.31$. Therefore, we find

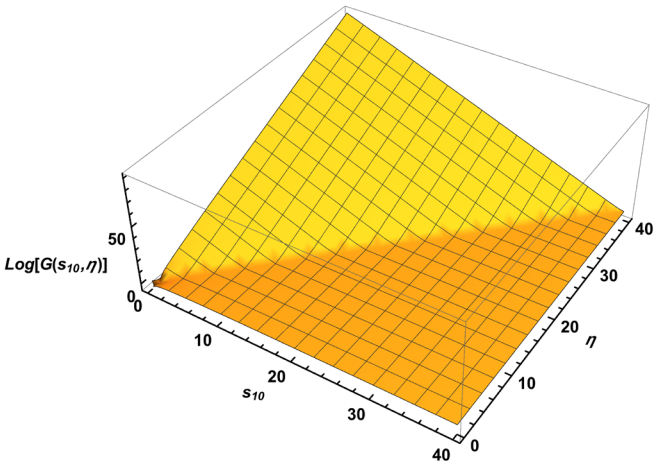

FIG. 1. The numerical solution of Eqs. (10) for the polarized dipole amplitude G plotted as a function of rescaled "rapidity" η and transverse variable s_{10}.

$$\Delta q^S(x,Q^2) \sim \Delta\Sigma(x,Q^2) \sim \left(\frac{1}{x}\right)^{\alpha_h} \quad (15)$$

with

$$\alpha_h = 2.31\sqrt{\frac{\alpha_s N_c}{2\pi}}, \quad (16)$$

where we have reinstated the factor $\sqrt{\alpha_s N_c/2\pi}$ originally scaled out by Eq. (9). (We also note that $\beta_h \approx -\alpha_h$.) Given that quarks can split into gluons at any step of evolution, we suspect that the gluon helicity PDF will have the same small-x intercept (16) but leave a rigorous calculation for future work. We mention that the uncertainty in α_h due to the choice of initial conditions and the extrapolation to the

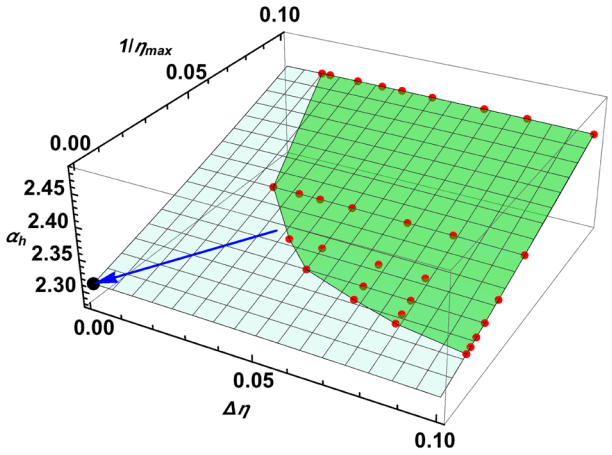

FIG. 2. Numerical results for our extraction of α_h. The "data" points are the intercepts we obtained for various $(\eta_{\max},\Delta\eta)$. The dark shaded piece of the plane indicates the region that is within our computational range, while the light area shows our extrapolation to the physical point $1/\eta_{\max} = \Delta\eta = 0$ (large solid dot).

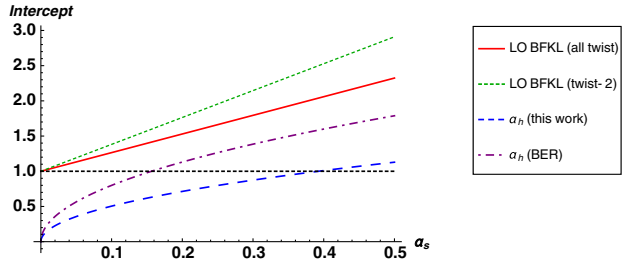

FIG. 3. Plot of the intercept vs α_s for helicity evolution (long-dashed and dot-dashed lines) and unpolarized LO BFKL evolution (solid and short-dashed lines). The long-dashed line shows the value of α_h extracted in this work for large N_c while the dot-dashed line gives that for the "pure glue" case of BER [19].

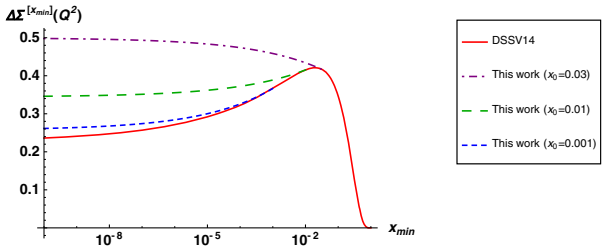

FIG. 4. Plot of $\Delta\Sigma^{[x_{\min}]}(Q^2)$ vs $x_{\min}$ at $Q^2 = 10$ GeV^2. The solid curve is from DSSV14 [41]. The dot-dashed, long-dashed, and short-dashed curves are from various small-x modifications of $\Delta\Sigma(x, Q^2)$ at $x_0 = 0.03$, 0.01, 0.001, respectively, using our helicity intercept (see the text for details).

physical point are both $< 1\%$ and negligible. This error is strictly from our current numerical analysis and does not include the impact on α_h that arises from including $N_f \neq 0$ as well as from next-to-leading order and running coupling corrections.

We note that the value in Eq. (16) is in disagreement with the "pure glue" intercept of $3.66\sqrt{\alpha_s N_c/2\pi}$ [38] obtained by BER [19] by about 35%. In Fig. 3, we compare these two intercepts along with that for unpolarized LO BFKL evolution (all twist and twist-2). Interestingly, the leading twist approximation to $\alpha_P - 1$ in BFKL evolution is larger than the exact all-twist intercept by about 30% [39]; it is possible something similar is occurring for helicity evolution. In Ref. [32], we have explored this possibility, performed various analytical cross-checks of our helicity evolution equations, and compared to BER where possible; we have not found any inconsistencies in our result.

Impact on the proton spin.—In order to determine the quark and gluon spin based on Eqs. (2), (3), one needs to extract the helicity PDFs. There are several groups who have performed such analyses, e.g., DSSV [40,41], JAM [42,43], LSS [44–46], NNPDF [47,48]. While the focus at small x has been on the behavior of $\Delta G(x, Q^2)$, there is actually quite a bit of uncertainty in the size of $\Delta\Sigma(x, Q^2)$ in that regime as well.

Let us define the truncated integral

$$\Delta\Sigma^{[x_{\min}]}(Q^2) \equiv \int_{x_{\min}}^{1} dx \Delta\Sigma(x, Q^2). \tag{17}$$

One finds for DSSV14 [41] that the central value of the full integral $\Delta\Sigma^{[0]}(10\ \text{GeV}^2)$ is about 40% smaller than $\Delta\Sigma^{[0.001]}(10\text{GeV}^2)$. The NNPDF14 [48] helicity PDFs lead to a similar decrease, although, due to the nature of neural network fits, the uncertainty in this extrapolation is 100%. On the other hand, for JAM16 [43] helicity PDFs the decrease from the truncated to the full integral of $\Delta\Sigma(x, Q^2)$ seems to be at most a few percent. The origin of this uncertainty, and more generally, the behavior of $\Delta\Sigma(x, Q^2)$ at small x, is mainly due to varying predictions for the size and shape of the sea helicity PDFs, in particular, $\Delta s(x, Q^2)$ [40–43,47–49]. So far, the only constraint on $\Delta s(x, Q^2)$, and how it evolves at small x, comes from the weak neutron and hyperon decay constants. Therefore, there is a definite need for direct input from theory on the small-x intercept of $\Delta\Sigma(x, Q^2)$: this is what we have provided in this Letter.

We now will attempt to quantify how the small-x behavior of $\Delta\Sigma(x, Q^2)$ derived here affects the integral in Eq. (2). We take a simple approach and leave a more rigorous phenomenological study for future work. First, we attach a curve $\Delta\tilde{\Sigma}(x, Q^2) = Nx^{-\alpha_h}$ [with α_h given in (16)] to the DSSV14 result for $\Delta\Sigma(x, Q^2)$ at a particular small-x point x_0. Next, we fix the normalization N by requiring $\Delta\tilde{\Sigma}(x_0, Q^2) = \Delta\Sigma(x_0, Q^2)$. Finally, we calculate the truncated integral (17) of the modified quark helicity PDF

$$\Delta\Sigma_{\text{mod}}(x, Q^2) \equiv \theta(x - x_0)\Delta\Sigma(x, Q^2) + \theta(x_0 - x)\Delta\tilde{\Sigma}(x, Q^2) \tag{18}$$

for different x_0 values. The results are shown in Fig. 4 for $Q^2 = 10$ GeV^2 and $\alpha_s \approx 0.25$, in which case $\alpha_h \approx 0.80$.

We see that the small-x evolution of $\Delta\Sigma(x, Q^2)$ could offer a moderate to significant enhancement to the quark spin, depending on where in x the effects set in and on the parametrization of the helicity PDFs at higher x. Thus, it will be important to incorporate the results of this work, and more generally, the small-x helicity evolution equations discussed here, into future extractions of helicity PDFs that include data at smaller x from an Electron-Ion Collider.

Conclusion.—In this Letter, we have numerically solved the small-x helicity evolution equations of Ref. [31] in the large-N_c limit. We found an intercept of $\alpha_h = 2.31\sqrt{\alpha_s N_c/2\pi}$, which, from Eq. (15), is a direct input from theory on the behavior of $\Delta\Sigma(x, Q^2)$ at small x. Although a more rigorous phenomenological study is needed, we demonstrated in a simple approach that such an intercept could offer a moderate to significant enhancement of the quark contribution to the proton spin. Therefore, it appears imperative to include the effects of

the small-x helicity evolution discussed here in future fits of helicity PDFs, especially those to be obtained at an Electron-Ion Collider.

We thank S. Mukherjee for useful discussions on analyzing the numerical results. We thank R. Sassot and W. Vogelsang for providing us with the parameters and FORTRAN code of the DSSV14 fit. We are also grateful to R. Furnstahl, A. Metz, B. Schenke, and J. Stapleton for useful conversations. This material is based upon work supported by the U.S. Department of Energy, Office of Science, Office of Nuclear Physics under Award No. DE-SC0004286 (YK) and within the framework of the TMD Topical Collaboration (DP) and DOE Contract No. DE-SC0012704 (MS). DP also received support from the RIKEN BNL Research Center. MS received additional support from an EIC program development fund from BNL and from the U.S. Department of Energy, Office of Science under the DOE Early Career Program.

*kovchegov.1@osu.edu
†dap67@psu.edu
‡sievertmd@lanl.gov

[1] R. L. Jaffe and A. Manohar, Nucl. Phys. **B337**, 509 (1990).
[2] X. D. Ji, Phys. Rev. Lett. **78**, 610 (1997).
[3] X. Ji, X. Xiong, and F. Yuan, Phys. Rev. Lett. **109**, 152005 (2012).
[4] There has been much work in the literature on the decomposition of the proton's spin (see Ref. [5] for a review).
[5] E. Leader and C. Lorcé, Phys. Rep. **541**, 163 (2014).
[6] J. Ashman *et al.* (European Muon Collaboration), Phys. Lett. B **206**, 364 (1988).
[7] J. Ashman *et al.* (European Muon Collaboration), Nucl. Phys. **B328**, 1 (1989).
[8] L. Adamczyk *et al.* (STAR Collaboration), Phys. Rev. Lett. **115**, 092002 (2015).
[9] A. Adare *et al.* (PHENIX Collaboration), Phys. Rev. D **93**, 011501 (2016).
[10] We refer the reader to Refs. [11–13] for a more comprehensive overview of the current situation.
[11] A. Accardi *et al.*, Eur. Phys. J. A **52**, 268 (2016).
[12] E. C. Aschenauer *et al.*, arXiv:1304.0079.
[13] E. C. Aschenauer *et al.*, arXiv:1501.01220.
[14] R. Kirschner and L. n. Lipatov, Nucl. Phys. **B213**, 122 (1983).
[15] R. Kirschner, Z. Phys. C **65**, 505 (1995).
[16] R. Kirschner, Z. Phys. C **67**, 459 (1995).
[17] S. Griffiths and D. A. Ross, Eur. Phys. J. C **12**, 277 (2000).
[18] J. Bartels, B. I. Ermolaev, and M. G. Ryskin, Z. Phys. C **70**, 273 (1996).
[19] J. Bartels, B. I. Ermolaev, and M. G. Ryskin, Z. Phys. C **72**, 627 (1996).
[20] A. H. Mueller, Nucl. Phys. **B415**, 373 (1994).
[21] A. H. Mueller and B. Patel, Nucl. Phys. **B425**, 471 (1994).
[22] A. H. Mueller, Nucl. Phys. **B437**, 107 (1995).
[23] I. Balitsky, Nucl. Phys. **B463**, 99 (1996).
[24] I. Balitsky, Phys. Rev. D **60**, 014020 (1999).
[25] Y. V. Kovchegov, Phys. Rev. D **60**, 034008 (1999).
[26] Y. V. Kovchegov, Phys. Rev. D **61**, 074018 (2000).
[27] J. Jalilian-Marian, A. Kovner, and H. Weigert, Phys. Rev. D **59**, 014015 (1998).
[28] J. Jalilian-Marian, A. Kovner, A. Leonidov, and H. Weigert, Phys. Rev. D **59**, 014014 (1998).
[29] E. Iancu, A. Leonidov, and L. D. McLerran, Phys. Lett. B **510**, 133 (2001).
[30] E. Iancu, A. Leonidov, and L. D. McLerran, Nucl. Phys. **A692**, 583 (2001).
[31] Y. V. Kovchegov, D. Pitonyak, and M. D. Sievert, J. High Energy Phys. 01 (2016) 072.
[32] Y. V. Kovchegov, D. Pitonyak, and M. D. Sievert, Phys. Rev. D **95**, 014033 (2017).
[33] There is also a TMD version of Eq. (5) written down in Eq. (8c) of Ref. [32].
[34] The large-N_c limit with LLA saturation corrections included can be found in Eqs. (80), (82) of Ref. [31]. The large-N_c & N_f version of those formulas can be found in Eqs. (87)–(91) [or in Eqs. (92a)–(92c), (93a)–(93b) for the strict DLA form].
[35] Note that $G(x_{10}^2, z)$ has a sign opposite to that of the spin asymmetry defined in Eq. (A9) of Ref. [31]. This is analogous to the unpolarized case, where the Wilson line correlator is equal to $1 - N(x_{10}^2, z)$, where $N(x_{10}^2, z)$ is the imaginary part of the forward dipole–target scattering amplitude and has the same sign as the total cross section.
[36] We note that the procedure outlined below correctly reproduces the Reggeon intercept found in Ref. [37].
[37] K. Itakura, Y. V. Kovchegov, L. McLerran, and D. Teaney, Nucl. Phys. **A730**, 160 (2004).
[38] This intercept is for finite N_c, but we also checked that the value does not change in the limit of large N_c.
[39] Y. V. Kovchegov and E. Levin, *Quantum Chromodynamics at High Energy* (Cambridge University Press, Cambridge, 2012).
[40] D. de Florian, R. Sassot, M. Stratmann, and W. Vogelsang, Phys. Rev. D **80**, 034030 (2009).
[41] D. de Florian, R. Sassot, M. Stratmann, and W. Vogelsang, Phys. Rev. Lett. **113**, 012001 (2014).
[42] P. Jimenez-Delgado, A. Accardi, and W. Melnitchouk, Phys. Rev. D **89**, 034025 (2014).
[43] N. Sato, W. Melnitchouk, S. E. Kuhn, J. J. Ethier, and A. Accardi (Jefferson Lab Angular Momentum Collaboration), Phys. Rev. D **93**, 074005 (2016).
[44] E. Leader, A. V. Sidorov, and D. B. Stamenov, Phys. Rev. D **73**, 034023 (2006).
[45] E. Leader, A. V. Sidorov, and D. B. Stamenov, Phys. Rev. D **82**, 114018 (2010).
[46] E. Leader, A. V. Sidorov, and D. B. Stamenov, Phys. Rev. D **91**, 054017 (2015).
[47] R. D. Ball *et al.* (NNPDF Collaboration), Nucl. Phys. **B874**, 36 (2013).
[48] E. R. Nocera *et al.* (NNPDF Collaboration), Nucl. Phys. **B887**, 276 (2014).
[49] E. C. Aschenauer, R. Sassot, and M. Stratmann, Phys. Rev. D **92**, 094030 (2015).